Research on Engineering Structures & Materials
journal homepage: http://jresm.org
Research Group

Research Article

Fatigue life prediction of steel bridge connections using fracture mechanics models

Warda Abdulla*[a], Craig Menzemer[b]

Department of Civil Engineering, The University of Akron, U.S.A.

Article Info

Article history:
Received 10 Mar 2021
Revised 16 Jun 2021
Accepted 16 Jun 2021

Keywords:

AFGROW models;
Crack growth rate;
Fatigue life prediction;
Riveted connections;
Stress intensity factor;
Striation spacing

Abstract

Riveted connections used in steel bridges may be subjected to localized fatigue cracking. Experimental data were obtained from coupon fatigue tests for the investigation of the role of the riveting process on fatigue resistance. Fracture mechanics models of both open-hole and riveted A36 steel coupon specimens were used to predict the fatigue life. Stress versus the number of cycles to failure curves (S-N curves) were established based on empirical results and combined with Air Force Grow software (AFGROW) fatigue life estimates and compared. Fatigue crack growth test data was developed and compared with the material library in AFGROW. Fracture surfaces of the specimens were examined and striation spacing measured using Scanning Electron Microscope (SEM) images. Subsequently, stress intensity factors and local crack growth rates were estimated. Estimates of the local crack growth rates and the estimated stress intensity ranges were compared with data obtained from fatigue crack growth test results. Test results demonstrated that fatigue life was improved with the riveting process. In addition, accurate fatigue life predictions required consideration of the compressive residual stresses due to riveting.

1. Introduction

One particular design concern is the fluctuation of stress in a component which may cause localized fatigue cracking within a structural system. In general, it is necessary to consider all limit states of a component or structure which includes fatigue [1].

Fatigue cracking generally initiates as a result of localized cyclic plastic deformation, and starts with one or more tiny flaws in the material that grow sub critically until failure occurs. The idea is that even if the nominal stresses are well below the elastic limit, the local stresses may be above yield due to stress concentrations. It is worth noting that prevention of fracture is a significant aspect of design for structures that are subjected to repeated loading or vibration [1, 2].

Mechanically fastened structural connections commonly use either rivets or bolts. In fact, fasteners are often used in components of movable bridges such as in steel grid decks. Bridge decks are exposed to daily traffic load and one significant issue is the design against fatigue cracking induced by repeated cyclic loads. It is well known that connections under such conditions may eventually fail from fatigue cracking even though the maximum applied stress is less than the yield stress. In addition, these failures often occur with small

*Corresponding author: wia3@uakron.edu
[a] orcid.org/0000-0003-4549-4836; [b] orcid.org/0000-0002-6529-085X
DOI: http://dx.doi.org/10.17515/resm2021.264st0310

deformation, which makes fatigue cracks difficult to detect until major growth has occurred [3].

Consequently, fatigue life prediction must be considered during the design of structural components [4].

Fracture surfaces of components and test articles subjected to fatigue may contain striations, which represent locations of the crack front(s). Striations can help determine the direction of failure propagation, the local crack growth rate and may help identify the origin of failure. Further, correlations have been developed that establish the relationship between striation spacing or local crack growth rate da/dN and the stress intensity factor range (ΔK) [5, 6].

In order to understand the fatigue behavior of riveted joints and connections, experimental tests have been conducted and several models proposed over the years. The general idea of testing riveted joints and connections that use smaller rather than full-scale specimens, is simply that it is easier and less costly, but may be limited by scale effects [7].

Fatigue lives exhibit considerable scatter even under constant amplitude loading in controlled laboratory conditions. This phenomenon makes statistical methods indispensable. Further, fatigue life should be predicted at given probability levels of failure for a given detail under defined environment and loading conditions. Generally, the nominal applied stress range is the main parameter for fatigue life, and other loading parameters, such as the mean stress, have a minor effect [8].

Several different studies on the fatigue behavior of steel bridge connections have been performed using different types of analyses. Fatigue damage may also be associated with secondary load effects. Moreover, the interaction between bridge members and load-carrying systems has contributed to fatigue issues [9]. Furthermore, the discontinuities that exist in all fabricated steel structures are a consequence of the manufacturing process of the material and/or the normal fabrication processes of the components. These discontinuities from steel making, as well as various fabrication processes like cutting, drilling, punching, and welding operations provide preferential sites from which fatigue cracks may develop. Usually, lower fatigue resistance for welded joints is expected as compared with bolted or riveted details. It is worth noting that the fatigue behavior of fabricated steel structures is controlled by the detail type, size, shape, and location of the discontinuities, as well as the applied cyclic stresses [10].

As riveting is employed as a joining method in steel construction, fatigue tests and studies of riveted connections are of continued interest. Many of these studies use experimental, numerical, or theoretical analysis for the investigation of fatigue damage. To be specific, the main focus is the evaluation of fatigue life of either open-hole or riveted specimens. Researchers have studied crack initiation by testing open-hole specimens, and fatigue life determined as each specimen was tested to fracture. It has been found that crack growth in the open-hole specimens initiated almost exclusively at the edge of the hole. Thru thickness crack development around the edge of the hole appeared to be unsymmetrical in most cases [11]. The fatigue life of riveted sheet metal joints consisting of single as well as specimens with multiple fasteners was investigated. Fatigue testing was conducted on all specimen types and the analysis showed that connections using a stiffened angle design with either two or eight rivets was superior as compared to that of single lap joints with one and four rivets [12].

The goal of this study was to investigate the fatigue behavior of heavy-duty rivete steel grating under a standard AASHTO HL truck, although using coupon samples in order to understand the effect of riveting.

Two types of A36 steel specimens were employed and consisted of both open-hole and riveted samples with dog-bone geometry. The specimens were tested under different stress ranges until failure [13]. To provide a better understanding of the behavior of the riveted connection, fatigue life prediction using AFGROW was conducted. Moreover, the beneficial residual stresses resulting from the riveting process were taken into consideration in the AFGROW model [13]. Simulating the nature of the riveted connections in the bridge makes this study more realistic.

The open-hole and riveted fracture mechanics models considered in this study are described in detail. Fatigue test results of both the open-hole and riveted coupons subjected to different stress ranges are compared with the AFGROW fatigue life estimates. Fatigue crack growth tests were conducted, and life predictions derived and compared with AFGROW results using a tabular look-up model. Striation spacing measurements taken from four different areas of fracture surfaces of the tested samples were compared to fatigue crack growth test data. Fatigue crack growth rates for stress ratios (R) of 0.1 to 0.4 were derived for the open-hole and riveted models.

2. Fatigue Life Prediction Analysis

2.1. AFGROW Fracture Mechanics Models

2.1.1. General Background

AFGROW is a fracture mechanics-based software program originally developed by the U.S Air Force. AFGROW was originally developed for evaluating the residual strength and durability of aerospace components. AFGROW was transitioned to a commercial product and has undergone a number of revisions since first introduced. Capabilities include the analysis of crack development, growth, and fracture to predict the behavior of structural systems [14].

2.1.2. Fatigue Life Prediction

A convenient feature within the program is the user's ability to select material properties from a menu, which includes crack growth information. There are multiple models for representing crack growth kinetics. Several of the choices include the Tabular Look-Up and Harter-T methods, also the Forman, Walker, and NASGRO Equations. Crack growth rate data is provided as function of the stress intensity range, ΔK, ($\Delta K = K_{max} - K_{min}$) at a given stress ratio ($R = K_{min}/K_{max}$) for $R \geq 0.0$. In this study, we employed the NASGRO crack growth rate equation for fatigue life prediction as follows [14]:

$$\frac{da}{dN} = C\left[\left(\frac{1-f}{1-R}\right)\Delta K\right]^n \frac{\left(1-\frac{\Delta K_{th}}{\Delta K}\right)^p}{\left(1-\frac{K_{max}}{K_{crit}}\right)^q} \quad (1)$$

Where, da/dN is the fatigue crack growth rate, C is the crack growth constant, f is the crack opening function, R is the load ratio, ΔK is the stress intensity factor range, n, p, q are the empirical constants describing the behavior near the threshold, ΔK_{th} is the threshold stress intensity factor range for crack propagation and K_{crit} is the fracture toughness. It is noteworthy that Eq. (1) considers the three stages of fatigue crack growth, which is shown schematically by the curve in Figure 1. Region I is the fatigue threshold region, region II is the Paris region which described by the parameters C and n and region III represents

rapid-crack propagation while the fracture toughness, K_{crit} , determines the transition to unstable crack growth [15, 16].

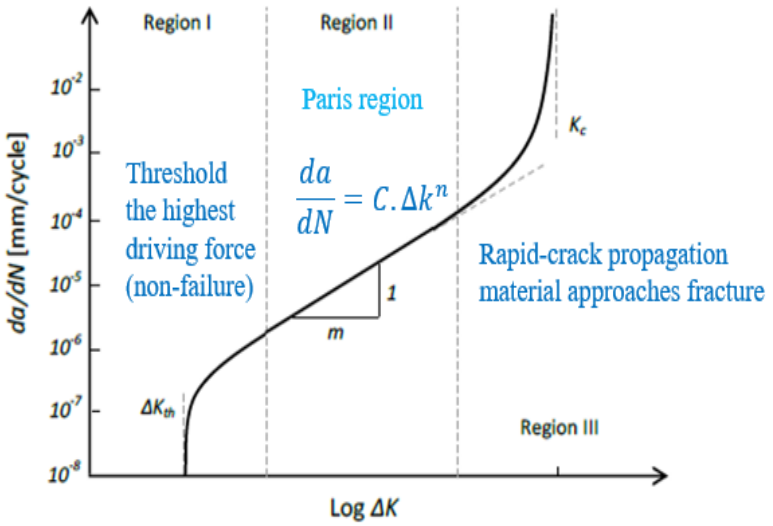

Fig. 1 Crack growth regions [16]

2.1.3 Modeling

A fracture mechanics model of a single corner crack at a hole was considered for the fatigue life prediction of the open-hole and the riveted coupon specimens. Two of the parameters considered included the stress ratio (R) and the a/c crack aspect ratio. The parameter a_i is the crack length and c_i is the crack depth. To check the model against the laboratory tests, the R-ratio was taken to be 0.1 for both coupon types [17].

2.1.3.1 Open-Hole Fracture Mechanics Model Inputs

The aspect ratio (a/c) for the open-hole coupon, was assumed to be between 0.15 and 0.29. The initial crack size (a_i) was assumed to be between (0.0254-0.1016 mm) and the crack depth (c_i) was assumed to be between (0.127-0.508 mm) [17].

2.1.3.2 Riveted Fracture Mechanics Model Inputs

For the riveted coupon specimens, the aspect ratio (a/c) was assumed to be between 0.15 and 0.3. The initial crack size (a_i) was assumed to vary between (0.0254-0.1016 mm) and the crack depth (c_i) was assumed to be between (0.127-0.508 mm). It is noteworthy that residual stress, an estimate of which was obtained from the finite element model analysis, was used as input to simulate the nature of the riveted sample [17]. This was as a result of the compression stress distribution obtained in the area of the corner crack, which has a positive influence on decreasing crack growth rates as reported in [13].

2.2. A comparison of AFGROW Calculated Results and Empirical Results

Regression analysis of the laboratory test data is compared with estimates calculated using AFGROW. Figure 2 shows both a lower bound and best-fit S-N curves for all of the study data along with AFGROW calculated results for the open hole configuration. In general, the results calculated using AFGROW are conservative as compared to the test results for lives greater than about 500,000 cycles. Also, design fatigue strength from both the lower bound

curve and equation 2 is 111 MPa at 10 million cycles, which is consistent with the experimental fatigue test results.

$$S_r = 70.965N^{-0.092} \quad (2)$$

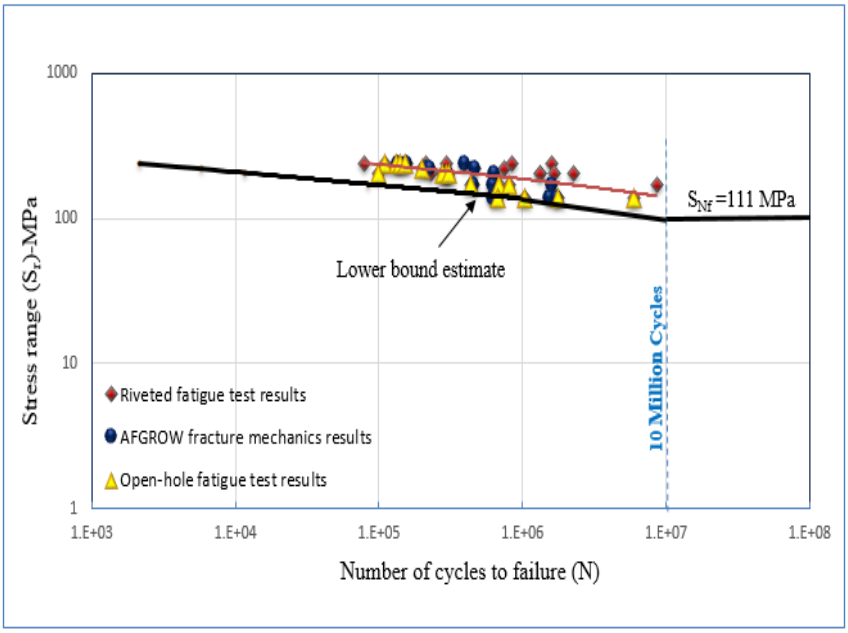

Fig. 2 Regression analysis of fracture mechanics and fatigue test results

Regression analysis of the laboratory test data is compared with estimates calculated using AFGROW. Figure 3 presents lower bound and best-fit S-N curves for all of the test data including the AFGROW results for the riveted configuration. Moreover, the design fatigue strength from both the lower bound curve and equation 3 is 113 MPa at 10 million cycles, which is slightly higher than the experimental fatigue test results.

$$S_r = 72.352N^{-0.092} \quad (3)$$

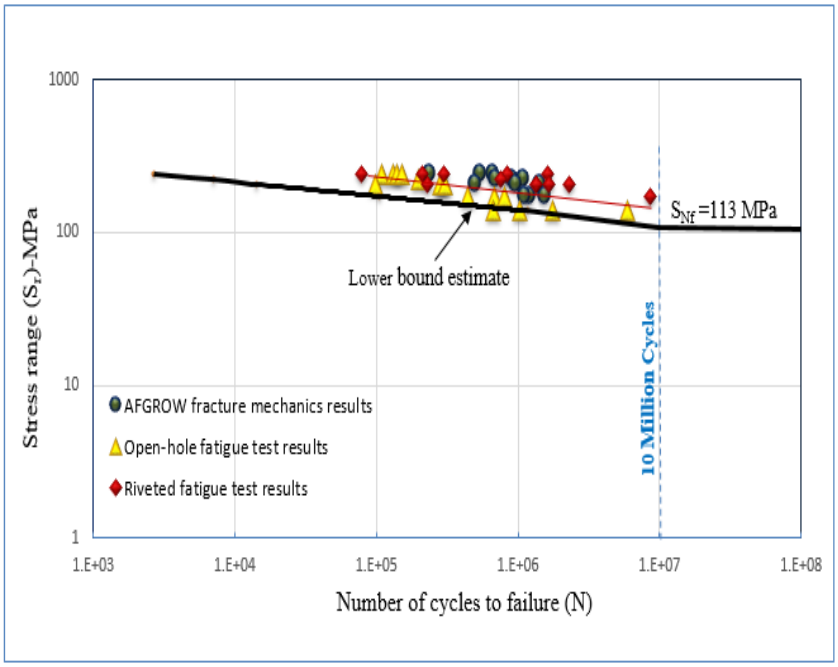

Fig. 3 Regression analysis of fracture mechanics and fatigue test results

3. Fatigue Crack Growth Rate Testing

Fatigue crack growth rate analysis helps designers to provide a safe lifetime, also it helps with the inspection process of critical components.

3.1. Fatigue Crack Growth Test Specimens

Fatigue crack growth analysis in the current study is based on A36 steel. The specimen configuration selected for examination is the single edge notched (SEN) depicted in Figure 4. All of the specimens had lengths of 152.4 mm, widths of 25.4 mm and thicknesses of 6.35 mm, with a notch size of 4.50 mm fabricated in the specimen. The advantage of the SEN is to concentrate stress in order to grow a crack from a controlled position. Further, it is relatively easy to fabricate and test.

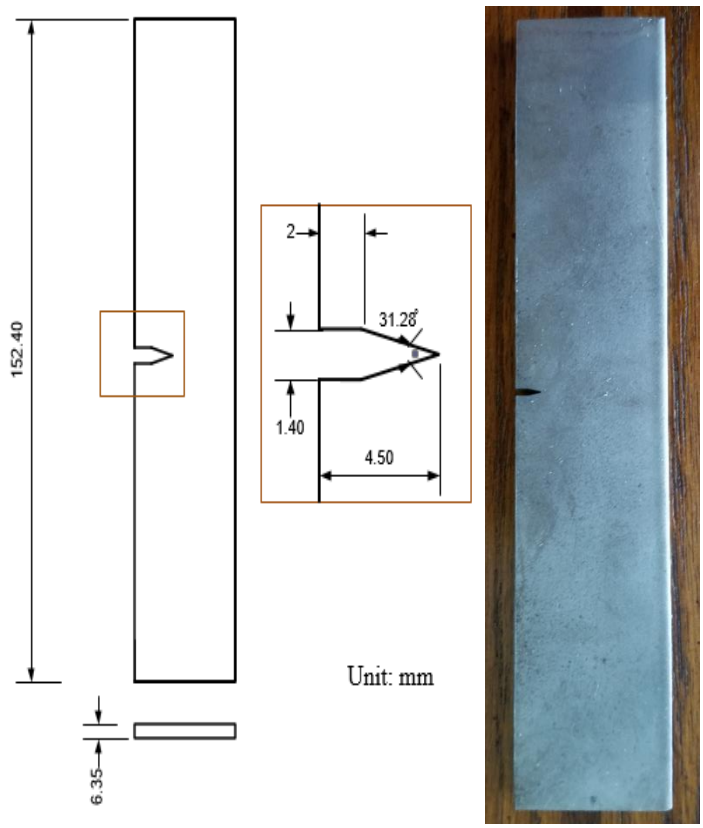

Fig. 4 Details of the single edge notched steel specimen

3.2. Experimental Setup

In order to simulate a natural fatigue crack, nine specimens were pre-cracked in tension. Also, the pre-crack helps ensure that the effect of the machined starter notch is removed from the specimen K-calibration and to obtain suitable test crack growth rate data [18].

Fatigue crack growth tests for nine specimens were conducted using an INSTRON machine with a 50 kN load cell. The specimen was gripped along the top and bottom sides using hydraulic wedge grips. Loading was applied at a frequency of 10 Hz in two steps:(a) the load magnitude was decreased 10% every 2000 cycles starting from 18 kN to obtain the K-decreasing portion close to the threshold and (b) the load was increased by 10% every 40,000 cycles starting from 18 to 26.6 kN to obtain K-increasing data.

The specimen was subjected to a direct current of 1 Amp through two leads using a Direct Current Potential Drop (DCPD) technique for crack monitoring. As the electrical resistivity changes, it reveals damage initiation and propagation. Consequently, an Agilent 34980a micro Ohmmeter was connected to the leads across the notch as shown in Figures 5 and 6 respectively. Data was recorded using two types of software Agilent and Wave Matrix.

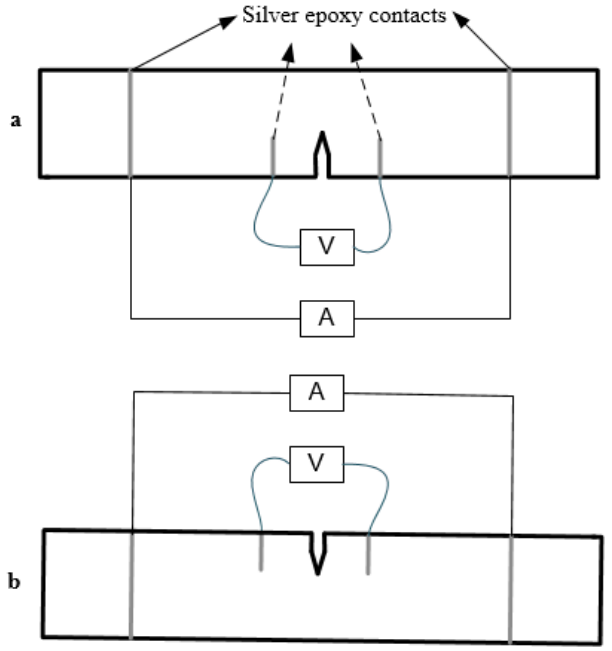

Fig. 5 Specimen configuration (a) front side (b) back side,

Note: A = Amps, V = Volts

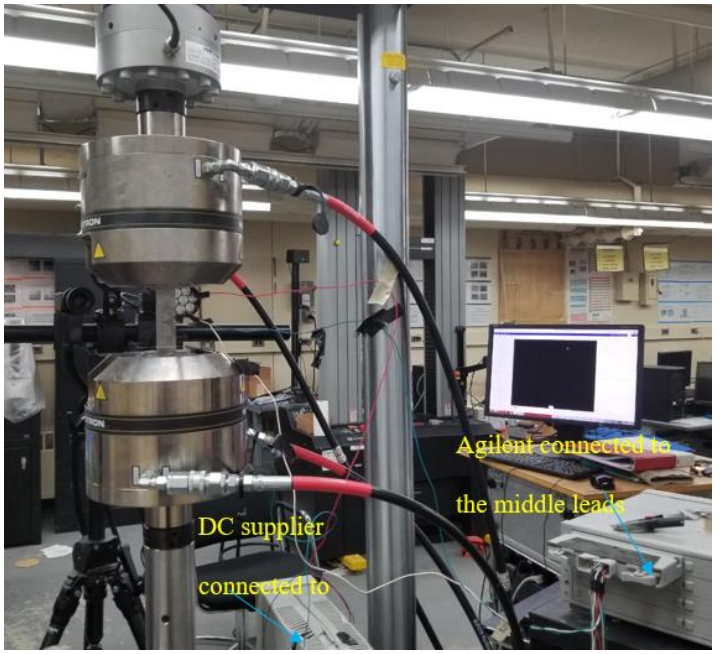

Fig. 6 Experimental setup with sensors position, ER and DC leads

3.3. Fatigue Crack Growth Test Results

The data was analyzed using MATLAB and Microsoft Excel, so crack length, time and number of cycles were obtained. The crack growth rate, defined as the change in length of a crack per cycle (da/dN) was calculated. Moreover, the stress intensity factor range (Δk) was calculated in order to correlate with the rate of fatigue crack growth using the following expression:

$$\Delta k = Y\Delta\sigma\sqrt{\pi a} \tag{4}$$

Where Y is a geometry factor, $\Delta\sigma$ is the stress range and a is the crack length.

Subsequently, Log (da/dN) is plotted versus Log (ΔK) and fatigue crack growth rates curve was obtained.

3.3.1. Crack Growth Rate vs. Stress Intensity Factor

Figure 7 presents the relationship between the crack growth rate and stress intensity factor range, which may conveniently be divided into three regions according to the curve shown below. In region I there is a threshold value, Δkth of 9.7 (MPa√m), below which cracks do not propagate, or the growth is too small to measure. It is worthwhile to mention that region I is sensitive to the effects of environment and stress ratio. In region II a linear relation between the Log (da/dN) and Log (ΔK) is commonly referred to as the Paris region. Region II behavior ranges from 11 to 50 (MPa√m). In region III, high values of ΔK are present, and there is rapid crack growth. Crack growth is limited by the material toughness, k_c.

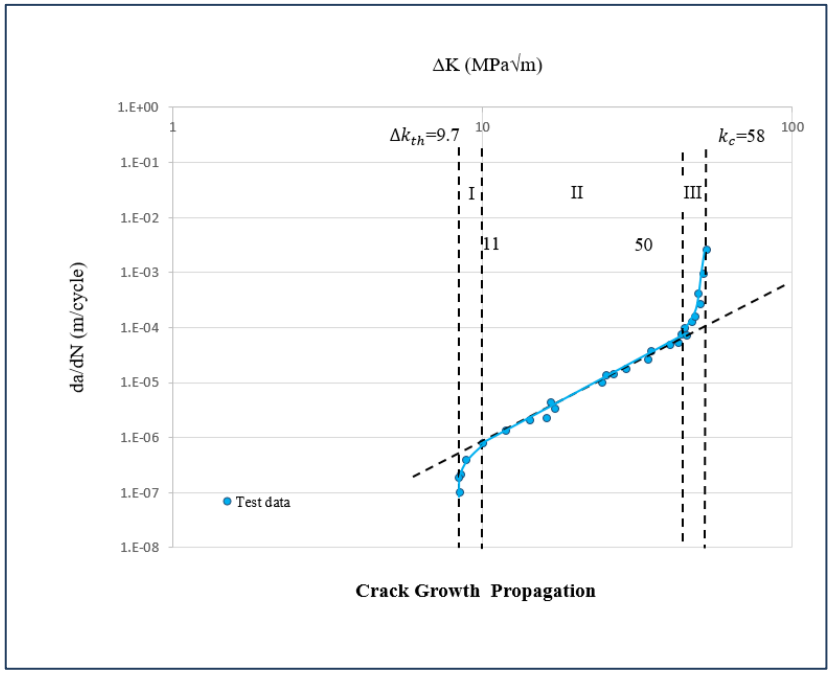

Fig. 7 Fatigue crack growth test results curve

3.3.2. A comparison of the Crack Growth Rates between the Experiments and AFGROW Modeling

Based on the experimental data shown on Figure 7, the fatigue threshold was estimated to be 9.7 (MPa√m), which is consistent with a value of 8.2 (MPa√m) used in the material library of AFGROW (Figure 8).

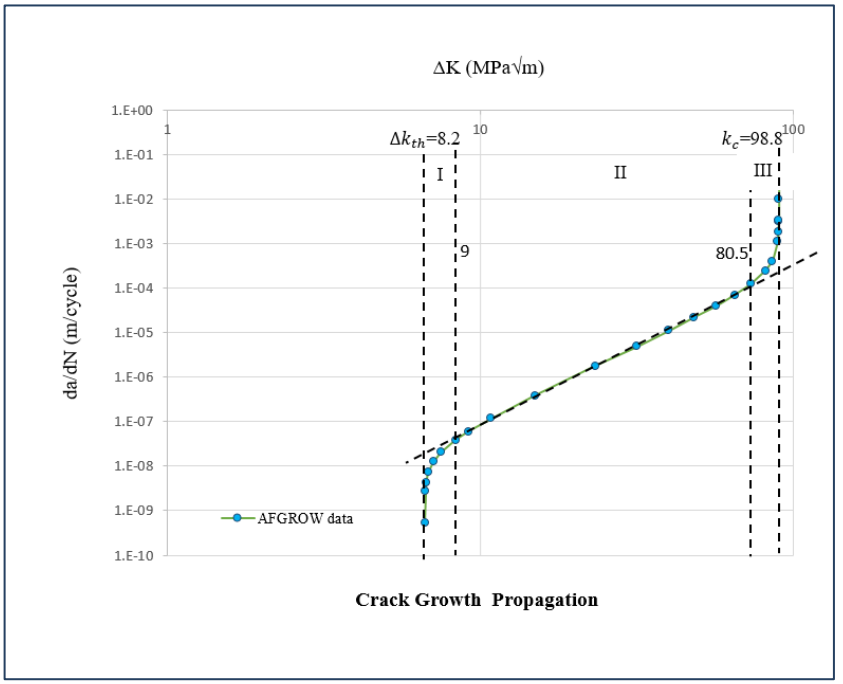

Fig. 8 Fracture mechanics crack growth curve

3.3.3. Comparison of Fatigue Crack Growth Test Results

Fatigue crack growth rate curves obtained from the laboratory tests were used as input to AFGROW using a tabular look-up model. Regression analysis of the fatigue test results is compared with estimates calculated using AFGROW. Figure 9 presents a best-fit S-N curve for the open-hole test data along with AFGROW calculated results.

Figure 10 shows a best-fit S-N curve for the riveted test data after adding AFGROW calculated results were for the riveted configuration, which was consistent as compared to the test results.

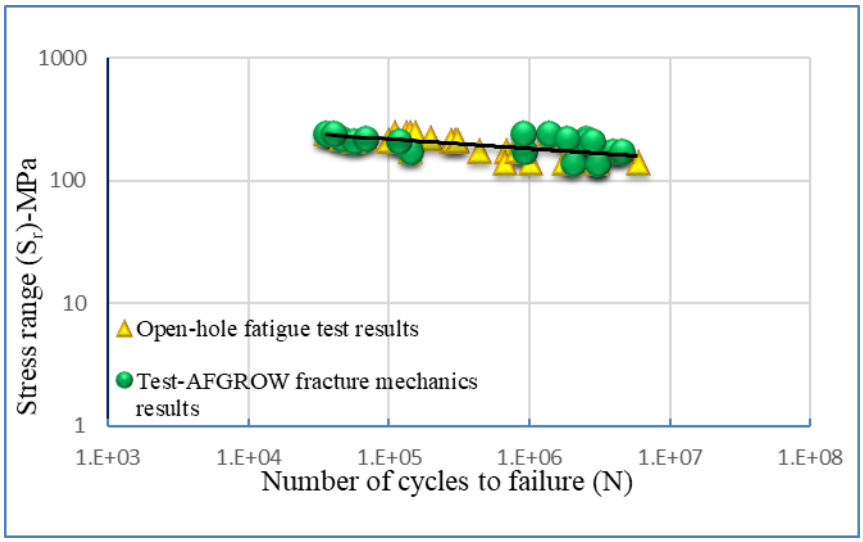

Fig. 9 Regression analysis of fracture mechanics and fatigue test results for the open-hole configuration

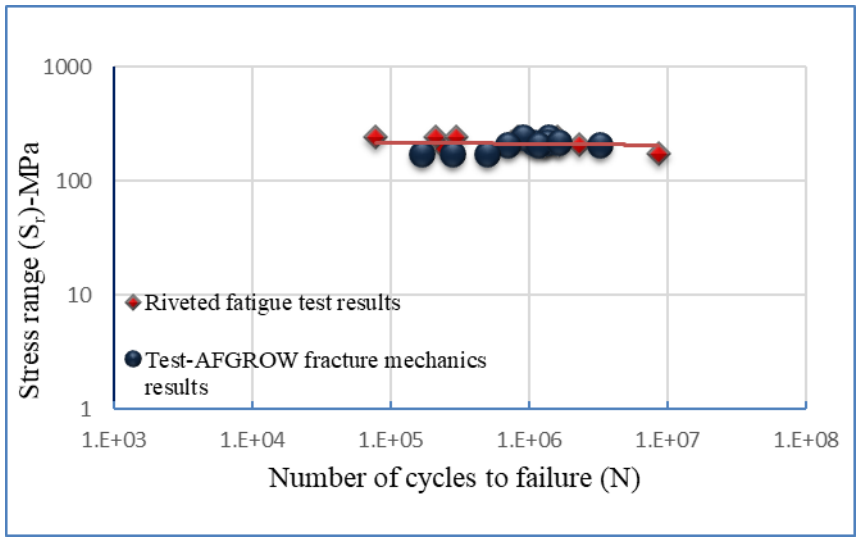

Fig. 10 Regression analysis of fracture mechanics and fatigue test results for the riveted configuration

4. Fatigue Striation Spacing Analysis

4.1. Inspection of Fracture Surfaces

Fatigue tests at a stress range of 206.8 MPa were performed on both open-hole and riveted samples. Fracture surfaces of the fully deformed and failed samples under fatigue loading were examined using Scanning Electron Microscope (SEM) [13].

4.2. A comparison of the Striation Spacing Between the Open-Hole and Riveted Coupons

Striations are features often produced on a fracture surface by fatigue crack growth in ductile materials. In fact, fatigue fracture surfaces are characterized by striations with small ridges perpendicular to crack propagation direction. Additionally, the striations develop at the crack tip because of the presence of slip that is inclined in relation to the fracture plane: when the load decreases, the slip direction turns. It is noteworthy that striations can help to determine the direction of failure propagation and the location of the origin. Striations may be observed and counted using images from the scanning electron microscope [19, 20].

One use of the striations is establishing the relationship between fatigue crack growth rate da/dN and stress intensity factor range (ΔK) [21]. Accordingly, spacing of striations were measured using SEM images (Figure 11). It is noteworthy that the fracture surfaces for each sample were divided into four different areas based on crack growth orientation to ensure accuracy of the spacing measurements. Consequently, stress intensity factors ranges were calculated for the open-hole and riveted samples as summarized in Table 1 and 2 respectively.

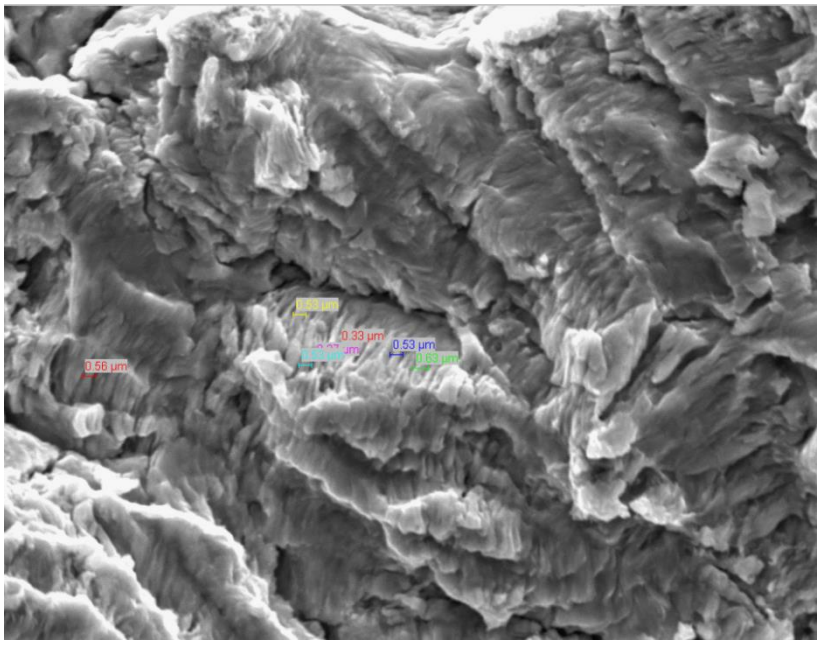

Fig. 11 Striation spacing measurements

Table 1. Fatigue crack growth rate measurements $\frac{da}{dN}$ $(\frac{m}{cycle})$ and estimated ΔK $(MPa\sqrt{m})$

Area	$\frac{da}{dN}$ $(\frac{m}{cycle})$	ΔK $(MPa\sqrt{m})$
1	5.08E-07	40.5
2	5.08E-07	40.5
3	5.842E-7	42.5
4	7.62E-07	46.4

Striation spacing, for the open-hole specimens vary from 5.08E-07 to 7.62E-07 $\frac{da}{dN}$ $(\frac{m}{cycle})$. Analogous stress intensity factors were calculated to range from 40.5to 46.4$(MPa\sqrt{m})$.

Table 2. Fatigue crack growth rate measurements $\frac{da}{dN}$ $(\frac{im}{cycle})$ and estimated ΔK $(MPa\sqrt{m})$

Area	$\frac{da}{dN}$ $(\frac{m}{cycle})$	ΔK $(MPa\sqrt{m})$
1	3.81E-07	36.8
2	4.06E-07	37.6
3	3.68E-07	36.4
4	3.76E-07	36.7

Also, striation spacing, for the riveted specimens in a similar location vary from 3.68E-07 to 4.06E-07 $\frac{da}{dN}$ $(\frac{m}{cycle})$. Corresponding stress intensity factors were calculated to range from 36.4 to 37.6$(MPa\sqrt{m})$. Generally, the size of a striation is related to the magnitude of the driving force characterized by the stress intensity factor. The striation`s width is indicative of the local crack growth rate. It might be noticed from the previous two tables that striation spacing for the riveted samples are narrower than they are for the open-hole samples. To be more specific, the riveted crack growth rates average is about 16% lower than the open-hole crack growth rates average. Furthermore, the average of the stress intensity factors of the riveted specimens is around 13% less than the open-hole stress intensity factors. It seems the rivet sample performs better, which demonstrates influence of the rivet as well as the installation process.

4.3. Correlations Between Crack Growth Rate and Stress Intensity Factor

Figure 12 compares fatigue crack growth rates for the open-hole specimens obtained from the SEM images along with fatigue crack growth test data. In region II, the crack growth rates as measured from the SEM data are consistent with the fatigue crack growth curve. Further, the highest value of ΔK obtained from the SEM data is 46.4$(MPa\sqrt{m}$, which is close to 50$(MPa\sqrt{m})$, the highest value of ΔK obtained from fatigue crack growth test data.

Figure 13 compares fatigue crack growth rates for the riveted specimens obtained from SEM images with fatigue crack growth test results. In region II, the crack growth rates were in reasonable agreement for the SEM and fatigue crack growth test results. Moreover, in

region II the highest value of stress intensity factor range, ΔK, obtained from SEM data is 37.6($MPa\sqrt{m}$, which is about 25% less than the highest value of ΔK obtained from fatigue crack growth test data. It appears the rivet influence improved the material behavior.

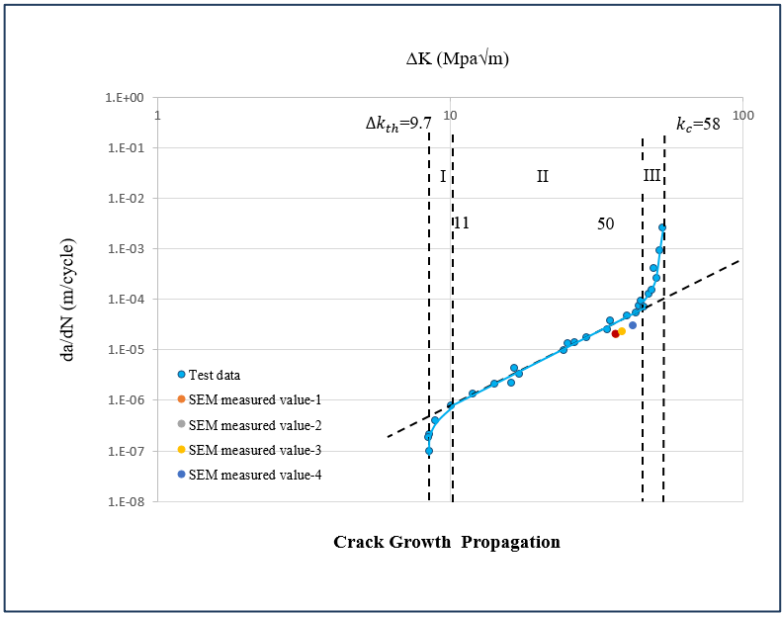

Fig. 12 Fatigue crack growth test results along with SEM open-hole data

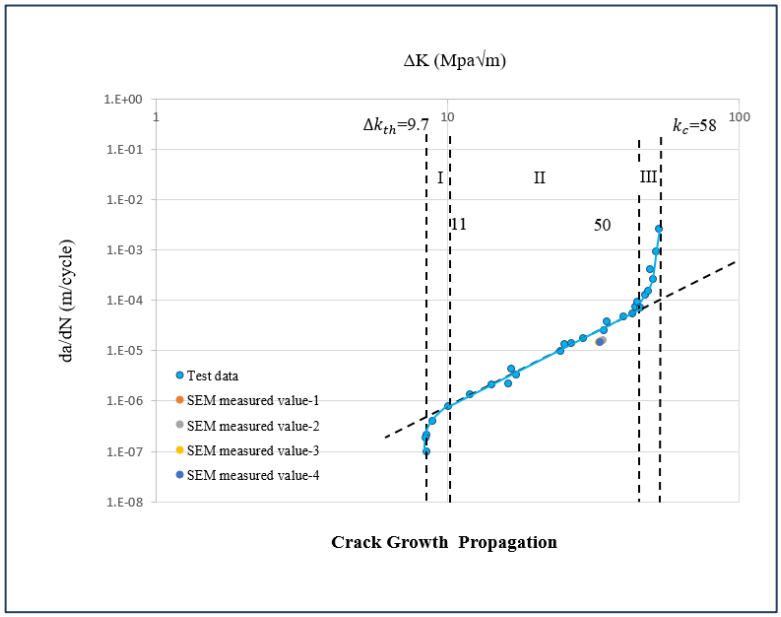

Fig. 13 Fatigue crack growth test results along with SEM riveted data

4.4. Correlations Between Crack Growth Rate and Stress Ratio Using AFGROW

Since fatigue cracks grow during the life of cyclically loaded components, any parameter which affects the growth can have a major effect on the total fatigue behavior of the components. One such parameter that has a significant effect on fatigue crack growth is stress ratio R [22, 23]. To account for the observed effect of stress ratio on crack growth rate, two different models have been proposed for the open-hole and riveted coupons. Generally, with increasing positive stress ratio at a given value of ΔK, the fatigue crack growth rate increases.

Figure 14 compares the influence of the R-ratio of 0.1 to 0.4 on the fatigue crack growth rate between the open-hole and the riveted specimens using AFGROW.

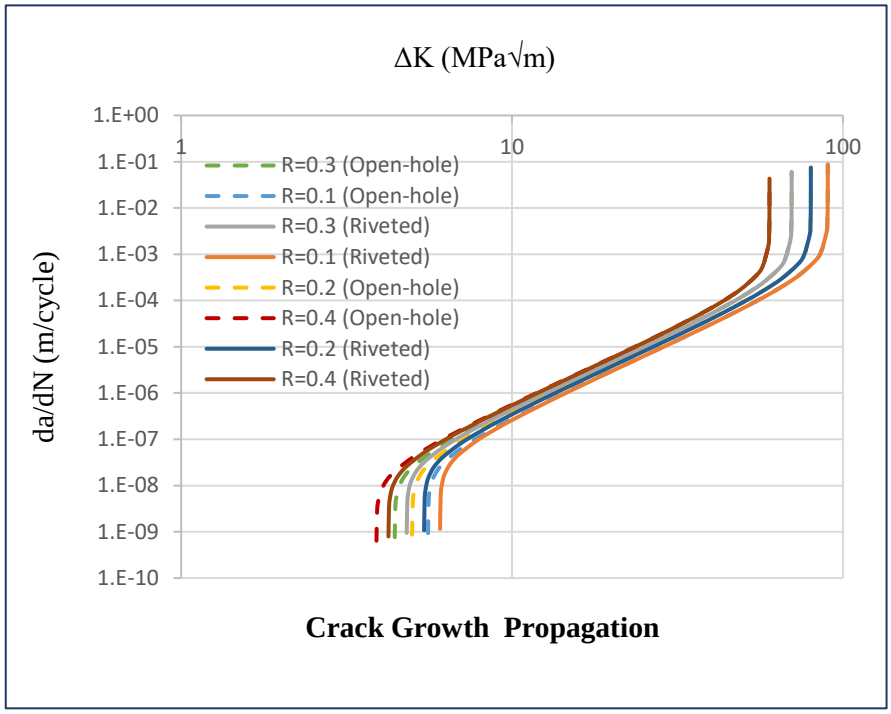

Fig. 14 Fatigue crack growth rate vs. stress intensity factor for different R-ratio

It might be seen that the effect of changing R-ratio for the open-hole and the riveted specimens is simply that the higher R-ratio increases crack growth rates and lowers fatigue life. However, the riveted samples exhibited longer fatigue life at stress ratio of 0.1as compared with the open hole, which demonstrates the positive effect of the rivet. It is important to note that the riveting process results in a compressive residual stress near the location of the origin of failure.

5. Conclusions

Fatigue has been a design consideration for open grid decks on bridges. In fact, some of the most replaced systems on movable bridges are the deck systems. As a result, fatigue life analysis and design of such systems are necessary. Within the scope of this study, fatigue

behavior of the deck focused on the riveted connections in heavy duty riveted steel grates. Therefore, fatigue test results for both open-hole and riveted coupons were compared with life predictions prepared using AFGROW. Fatigue life predictions were close to and consistent with the lower bound curves derived from open-hole test results. However, comparison of the predicted fatigue life of the riveted specimens using the fracture mechanics model shows that the predicted lives are slightly higher as compared to the test data. These results demonstrate the positive effect of the rivet and the residual stresses resulting from the riveting process.

Fatigue crack growth rate curves obtained from testing of the steel used in grate fabrication are conservative as compared with the corresponding simulations conducted using AFGROW. The Fatigue crack growth threshold based on the experimental test results was compared with the material library in AFGROW. The measured fatigue crack threshold was not identical to, but was similar to that from AFGROW. Based on the fracture mechanics models, the threshold stress intensity of the riveted specimen is about 17% greater than for the open-hole specimen at the same stress range. Reasonable agreement between the striation spacing measurements made from SEM images and the results of crack growth testing was observed. The best-fit S-N curve based on fatigue crack growth data analyzed by AFGROW using the tabular look-up model is in good agreement with the fatigue test results. The fatigue crack growth rate increases with increasing stress ratio at a given value of ΔK. The riveted specimens exhibited longer fatigue life, primarily due to the favorable residual stress field induced by the riveting process. This highlights the need to have a carefully controlled riveting process.

References

[1] Dowling NE. Mechanical behavior of materials: engineering methods for deformation, fracture, and fatigue. Pearson; 2012.
[2] Broek D. Elementary engineering fracture mechanics. Springer Science & Business Media; 2012.
[3] Kulak GL, Fisher JW, Struik JH. Guide to Design Criteria for Bolted and Riveted Joints Second Edition; 2001.
[4] Santecchia E, Hamouda AM, Musharavati F, Zalnezhad E, Cabibbo M, El Mehtedi M, Spigarelli S. A review on fatigue life prediction methods for metals. Advances in Materials Science and Engineering; 2016. https://doi.org/10.1155/2016/9573524
[5] Connors WC. Fatigue striation spacing analysis. Materials characterization. 1994 Oct 1; 33(3):245-53. https://doi.org/10.1016/1044-5803(94)90046-9
[6] Sbordone L, Traini T, Caputi S, Scarano A, Bortolaia C, Piattelli A. Scanning electron microscopy fractography analysis of fractured hollow implants. Journal of Oral Implantology. 2010 Apr; 36(2):105-11. https://doi.org/10.1563/AAID-JOI-D-10-90000
[7] Åkesson B. Fatigue life of riveted steel bridges. CRC Press; 2010. https://doi.org/10.1201/b10429
[8] Lassen T, Darcis P, Recho N. Fatigue Behavior of Welded Joints Part 1-Statistical Methods for Fatigue Life Prediction. Welding journal. 2005 Dec 1; 84(Suppl):183-7.
[9] Haghani R, Al-Emrani M, Heshmati M. Fatigue-prone details in steel bridges. Buildings. 2012 Dec; 2(4):456-76. https://doi.org/10.3390/buildings2040456
[10] Russo FM, Mertz DR, Frank KH, Wilson KE. Design and evaluation of steel bridges for fatigue and fracture-reference manual. National Highway Institute (US); 2016 Dec 1.

[11] Wang ZY, Li L, Liu YJ, Wang QY. Fatigue property of open-hole steel plates influenced by bolted clamp-up and hole fabrication methods. Materials. 2016 Aug; 9(8):698. https://doi.org/10.3390/ma9080698
[12] Urban MR. Analysis of the fatigue life of riveted sheet metal helicopter airframe joints. International journal of fatigue. 2003 Sep 1; 25(9-11):1013-26. https://doi.org/10.1016/j.ijfatigue.2003.08.003
[13] Abdulla W, Menzemer C. Fatigue Behavior of a Riveted Connection Detail Used in Steel Bridge Construction; 2020. https://doi.org/10.12988/ces.2020.91605
[14] Harter JA. AFGROW Reference Manual (version 5.3.3.23). Wright-Patterson Air Force Base, AFRL/VASM; 2019.
[15] Maierhofer J, Pippan R, Gänser HP. Modified NASGRO equation for physically short cracks. International Journal of fatigue. 2014 Feb 1; 59:200-7. https://doi.org/10.1016/j.ijfatigue.2013.08.019
[16] Blasón S, Correia JA, Apetre N, Arcari A, De Jesus AM, Moreira PM, Fernández-Canteli A. Proposal of a fatigue crack propagation model taking into account crack closure effects using a modified CCS crack growth model. Procedia Structural Integrity. 2016 Jan 1; 1:110-7. https://doi.org/10.1016/j.prostr.2016.02.016
[17] AFGROW, 5.03.05.22, crack growth life prediction software developed by LexTech, Inc., 2018.
[18] ASTM. Standard Test Method for Measurement of Fracture Toughness. E1820 - 18; 2018.
[19] Connors WC. Fatigue striation spacing analysis. Materials characterization. 1994 Oct 1; 33(3):245-53. https://doi.org/10.1016/1044-5803(94)90046-9
[20] Sbordone L, Traini T, Caputi S, Scarano A, Bortolaia C, Piattelli A. Scanning electron microscopy fractography analysis of fractured hollow implants. Journal of Oral Implantology. 2010 Apr; 36(2):105-11. https://doi.org/10.1563/AAID-JOI-D-10-90000
[21] Akhtar K, Khan SA, Khan SB, Asiri AM. Scanning electron microscopy: Principle and applications in nanomaterials characterization. InHandbook of materials characterization 2018 (pp. 113-145). Springer, Cham. https://doi.org/10.1007/978-3-319-92955-2_4
[22] Hudson CM, Scardina JT. Effect of stress ratio on fatigue-crack growth in 7075-T6 aluminum-alloy sheet. Engineering fracture mechanics. 1969 Apr 1; 1(3):429-46. https://doi.org/10.1016/0013-7944(69)90003-4
[23] Musuva JK, Radon JC. The effect of stress ratio and frequency on fatigue crack growth. Fatigue & Fracture of Engineering Materials & Structures. 1979 May; 1(4):457-70. https://doi.org/10.1111/j.1460-2695.1979.tb01333.x